

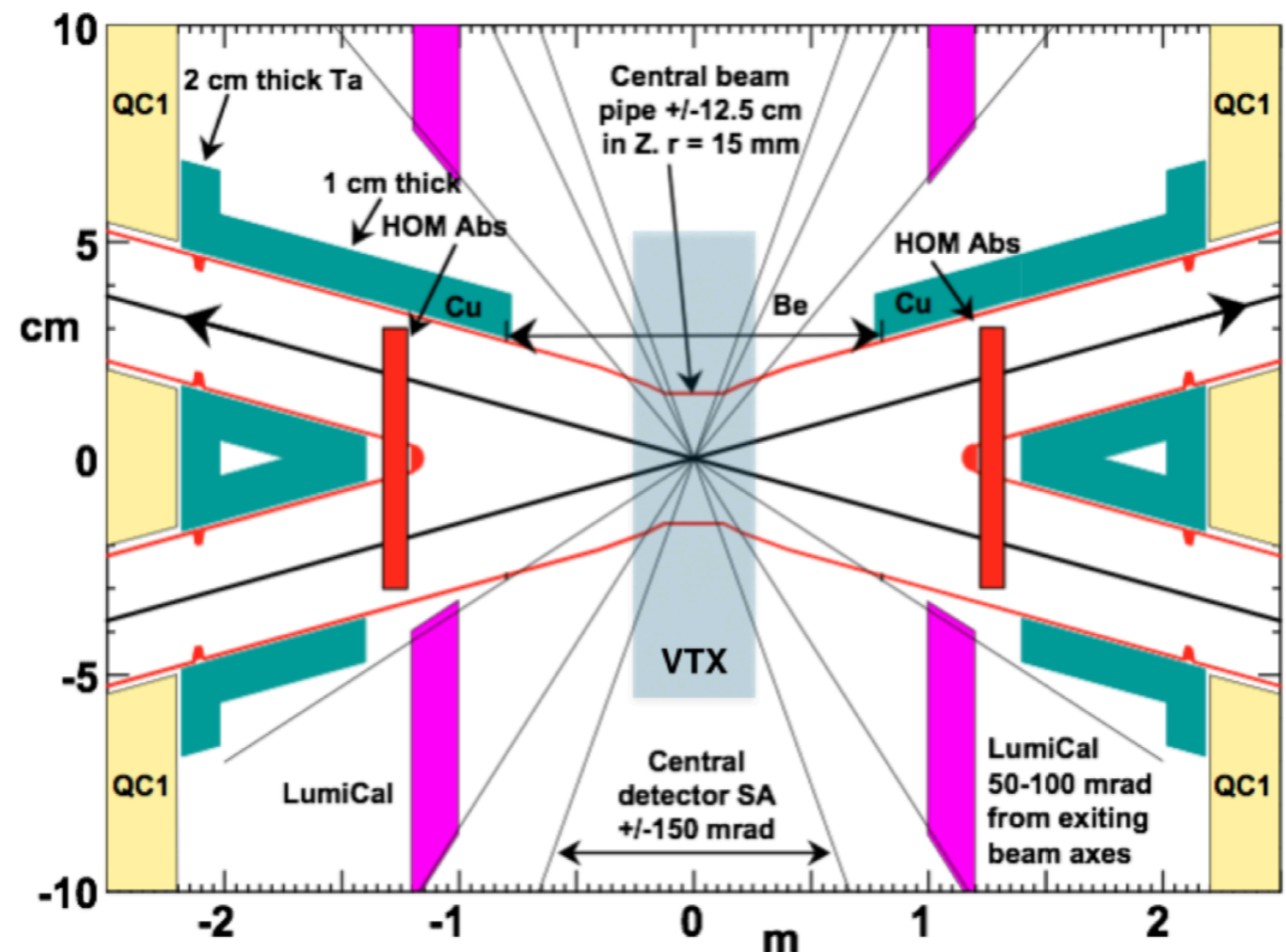
CLD detector performance with beam pipe with reduced diameter at IP - a first look -

*Emilia Leogrande (CERN),
on behalf of the CLICdp and FCC Collaborations*

FCC Week 2019
27/6/2019 - Brussels

- ◆ **CLD** (CLIC-Like Detector) is a detector concept developed for FCC-ee
- ◆ Design for the CDR (Dec 2018) **adapted from the CLICdet to the FCC-ee** interaction region specifics (crossing angle, magnets, beam pipe, background conditions)
- ◆ Performance satisfying the physics requirements [O. Viazlo's talk](#)

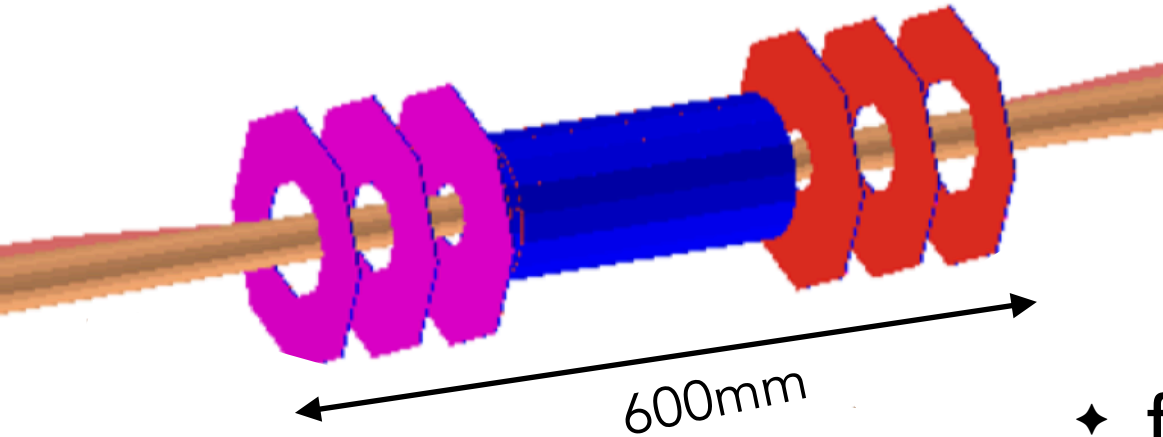
Concept	CLICdet	CLD
Vertex inner radius [mm]	31	17
Tracker half length [m]	2.2	
Tracker outer radius [m]	1.5	2.1
ECAL absorber	W	
ECAL X_0	22	
HCAL absorber	Fe	
HCAL λ_I	7.5	5.5
Solenoid field [T]	4	2
Overall height [m]	12.9	12.0
Overall length [m]	11.4	10.6



- ◆ **Novel design option post-CDR:**
 - ◆ **beam pipe at IP radius reduced from 15 mm to 10 mm**
 - ◆ CLD detector design adjusted to the new IR layout

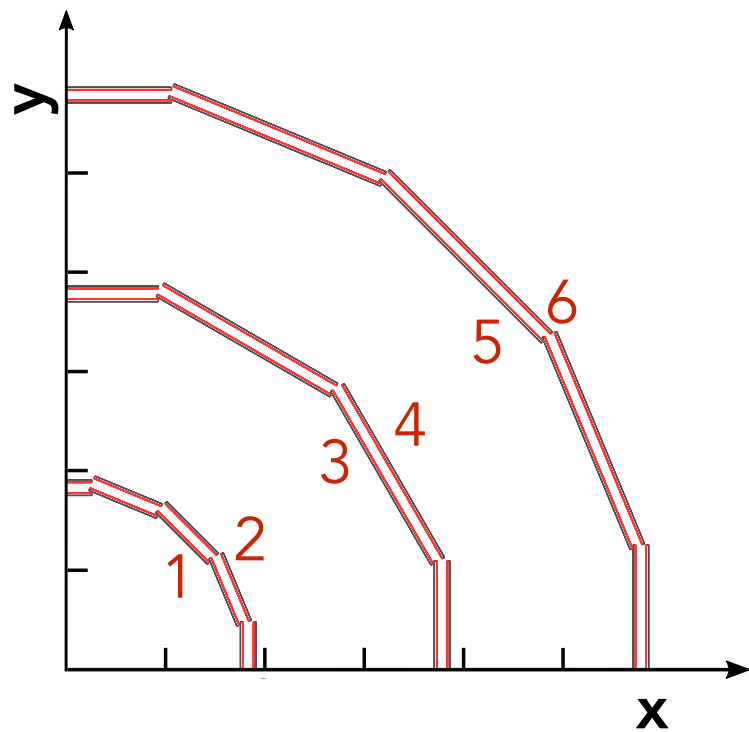


Vertex detector - design update



- ◆ 3 double barrel layers + 3 double layer disks per side
 - ◆ $0.6\%X_0$ per double layer
 - ◆ pixel size $25 \times 25 \mu\text{m}^2$
 - ◆ sensitive thickness $50 \mu\text{m}$ per layer

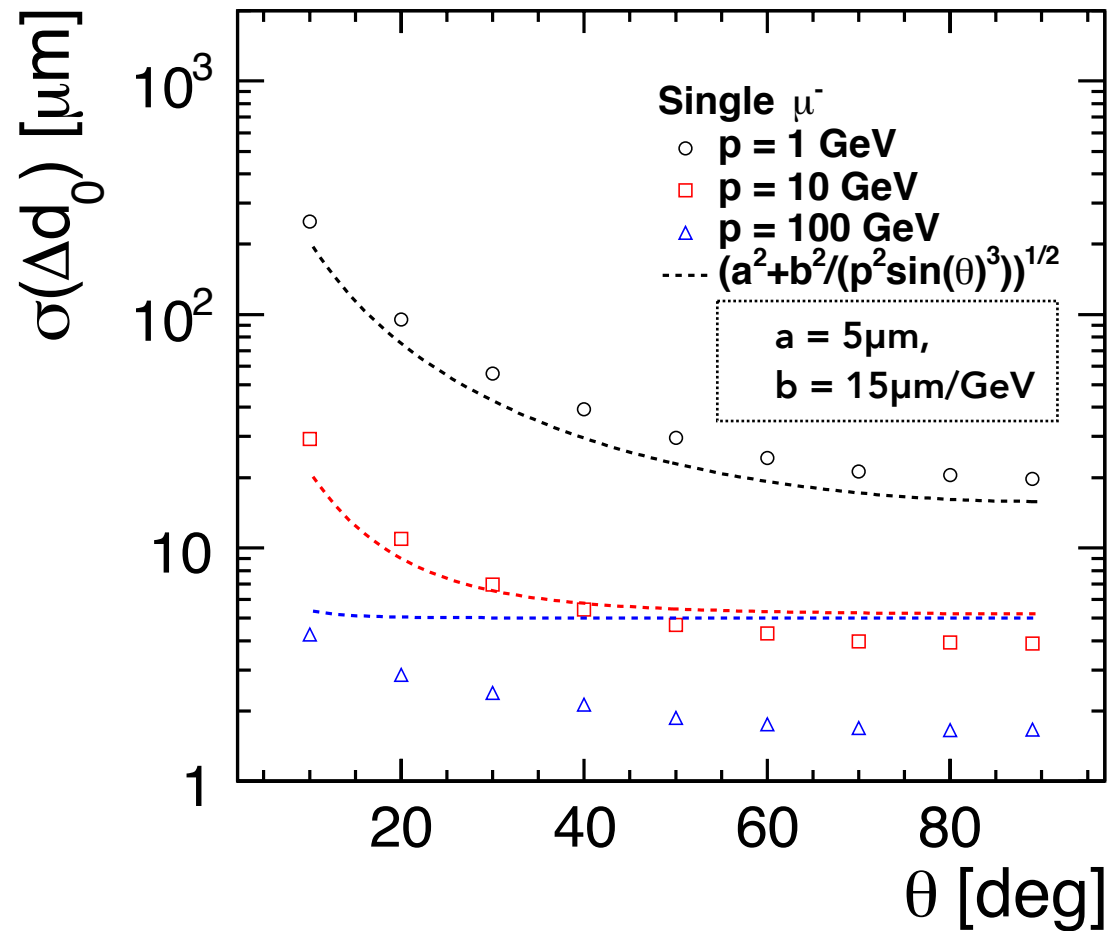
- ◆ **first double barrel layer closer to beam pipe**
- ◆ third barrel layer unchanged
- ◆ second barrel layer equidistant from first and third
- ◆ vertex disks unchanged



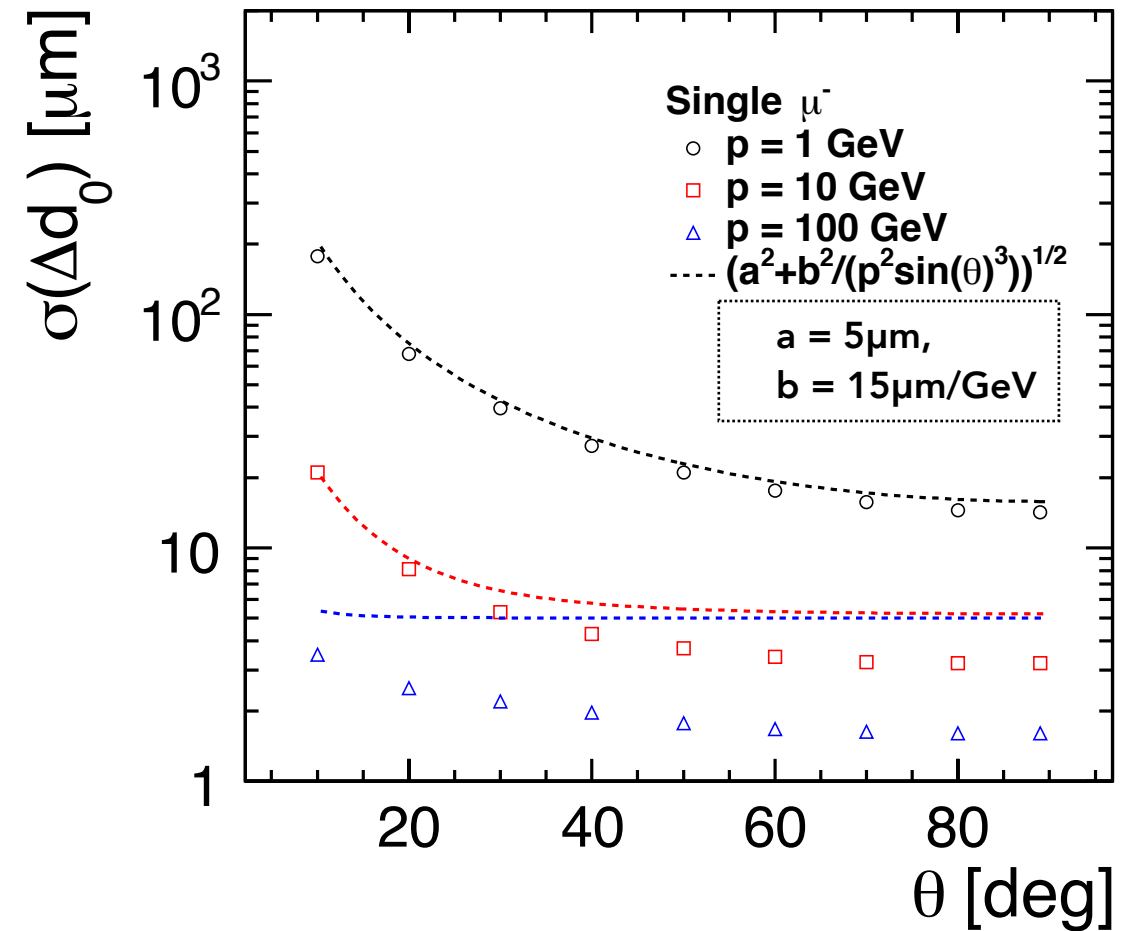
	CDR	post-CDR
beam pipe radius [mm]	15	10
r1 [mm]	17.5	12.5
r2 [mm]	18.5	13.5
r3 [mm]	37	35
r4 [mm]	38	36
r5 [mm]	57	57
r6 [mm]	58	58

- ◆ $\sigma(\Delta d_0)$ expected to improve with a vertex detector closer to the interaction point
- ◆ Results obtained in full detector simulation and reconstruction
- ◆ Resolution calculated as width of the Gaussian fit to the residual distribution per data point

CDR



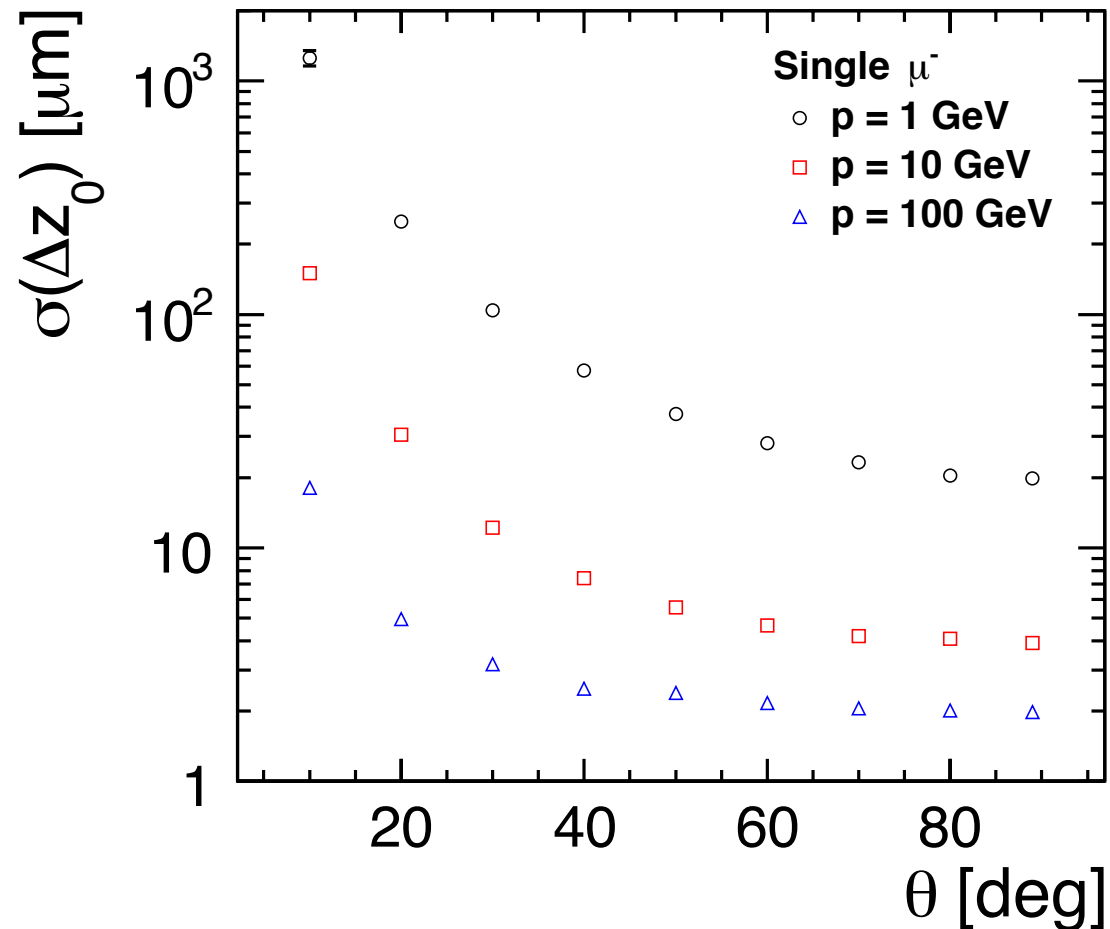
post-CDR



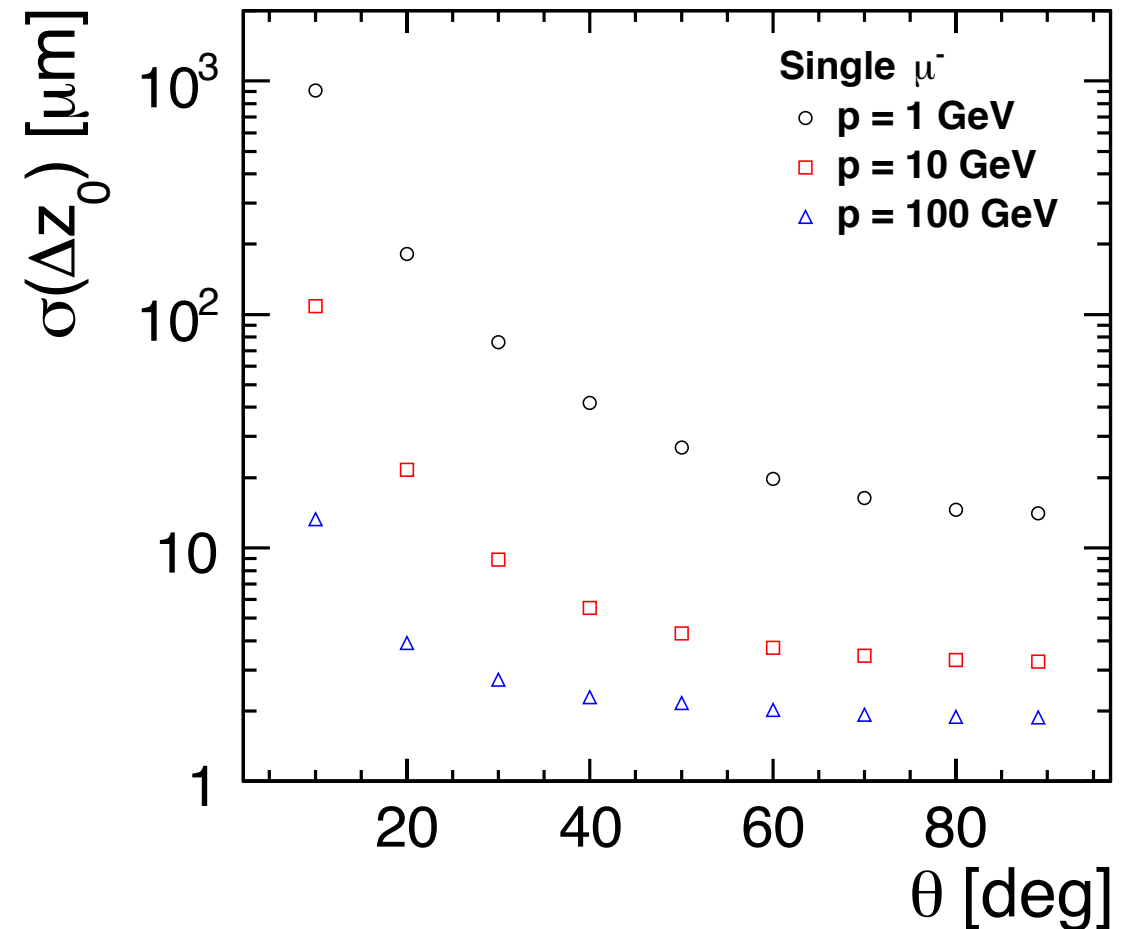
- ◆ improvement overall more visible for lower-energy muons
- ◆ resolution for muons with momentum of 1 GeV also matches the design goal

- ◆ $\sigma(\Delta z_0)$ expected to improve with a vertex detector closer to the interaction point
- ◆ Results obtained in full detector simulation and reconstruction
- ◆ Resolution calculated as width of the Gaussian fit to the residual distribution per data point

CDR

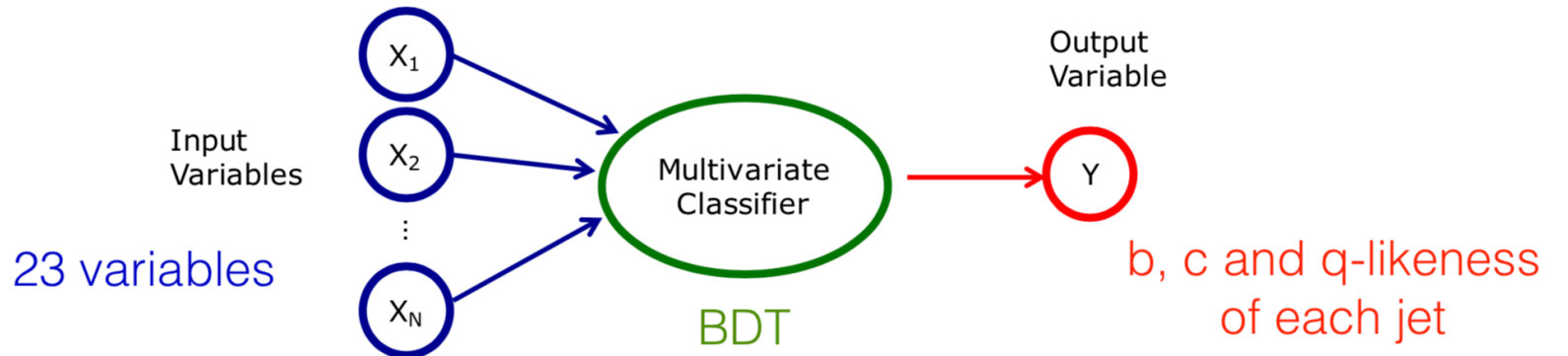


post-CDR



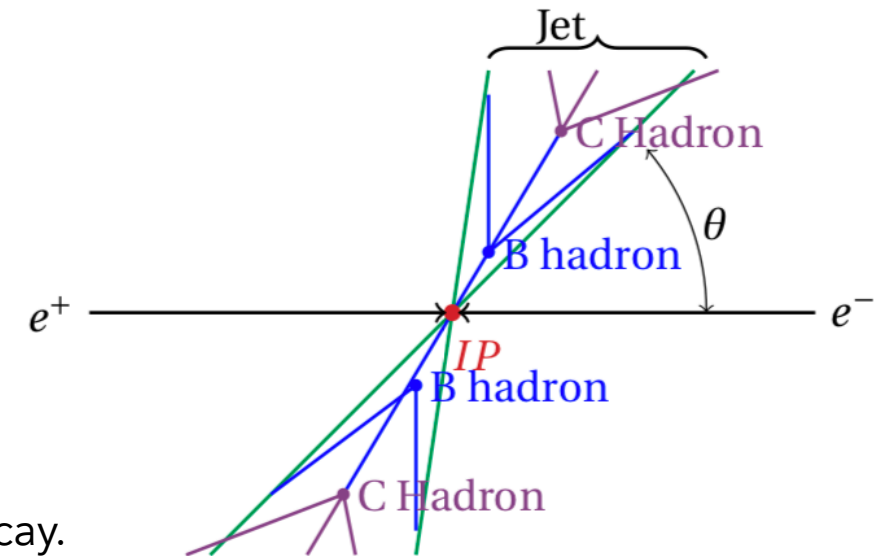
◆ improvement overall more significant for lower-energy muons

- ◆ Full simulation and reconstruction with LCFIPlus implemented in the Marlin framework of iLCSoft
- ◆ Algorithm chain:
 - ◆ vertex finder
 - ◆ jet clustering
 - ◆ vertex refiner
 - ◆ multivariate analysis



- ◆ dataset divided in 4 categories, used to train the BDT

Category	A	B	C	D
Number of vertices	0	1	1	2
Number of pseudovertrices*	0-2	0	1	0
	uds	c	b	



*pseudovertrices: b jets containing only one reconstructed secondary vertex with a possible track that could be interpreted as the result of an additional secondary decay. The cascade decays in a b jet are expected to result in decay points that are nearly collinear with the primary vertex. If only one secondary vertex is found, and if there is a track whose trajectory passes near a point collinear to the primary and secondary vertices, then the track is taken as a pseudo-vertex.

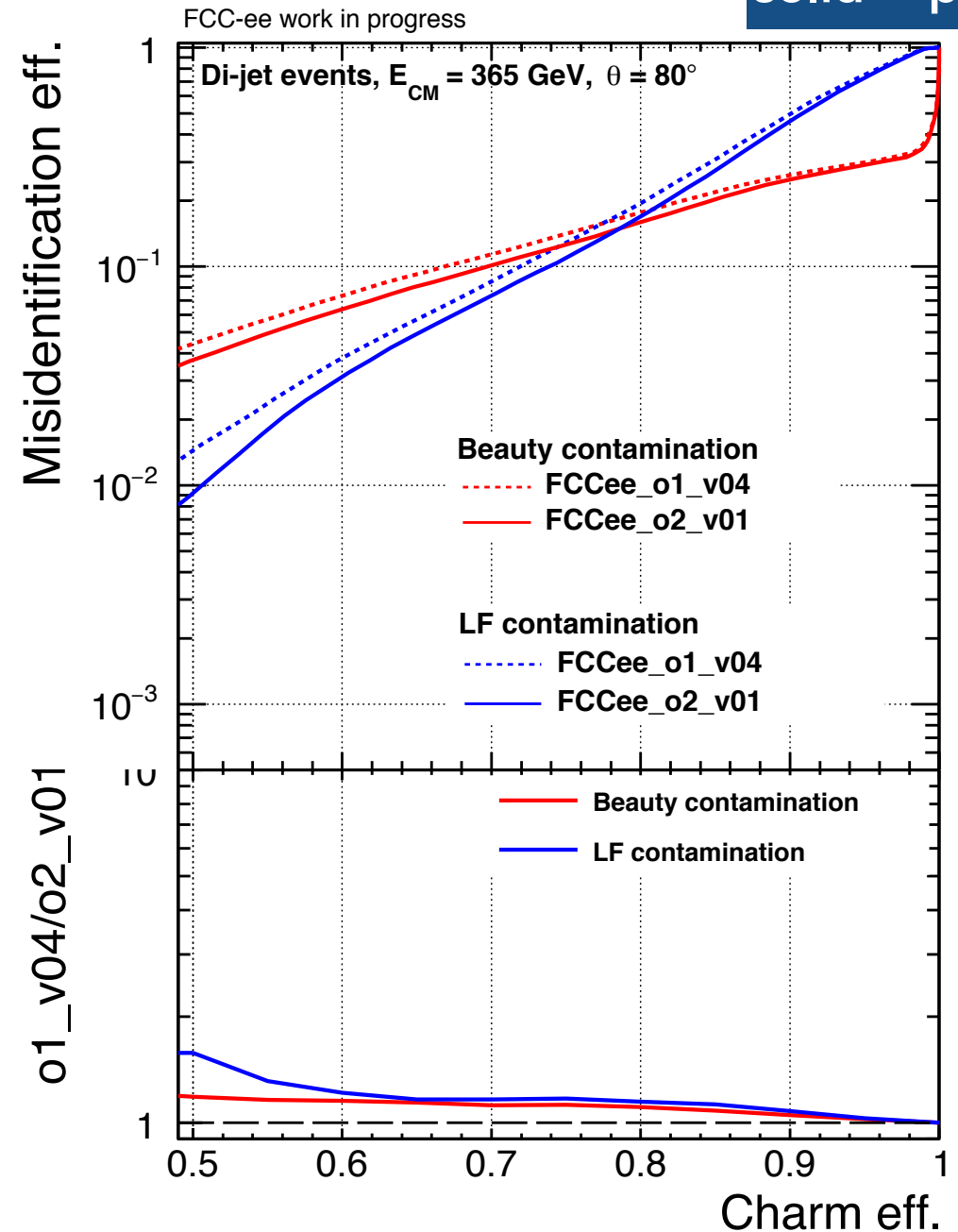
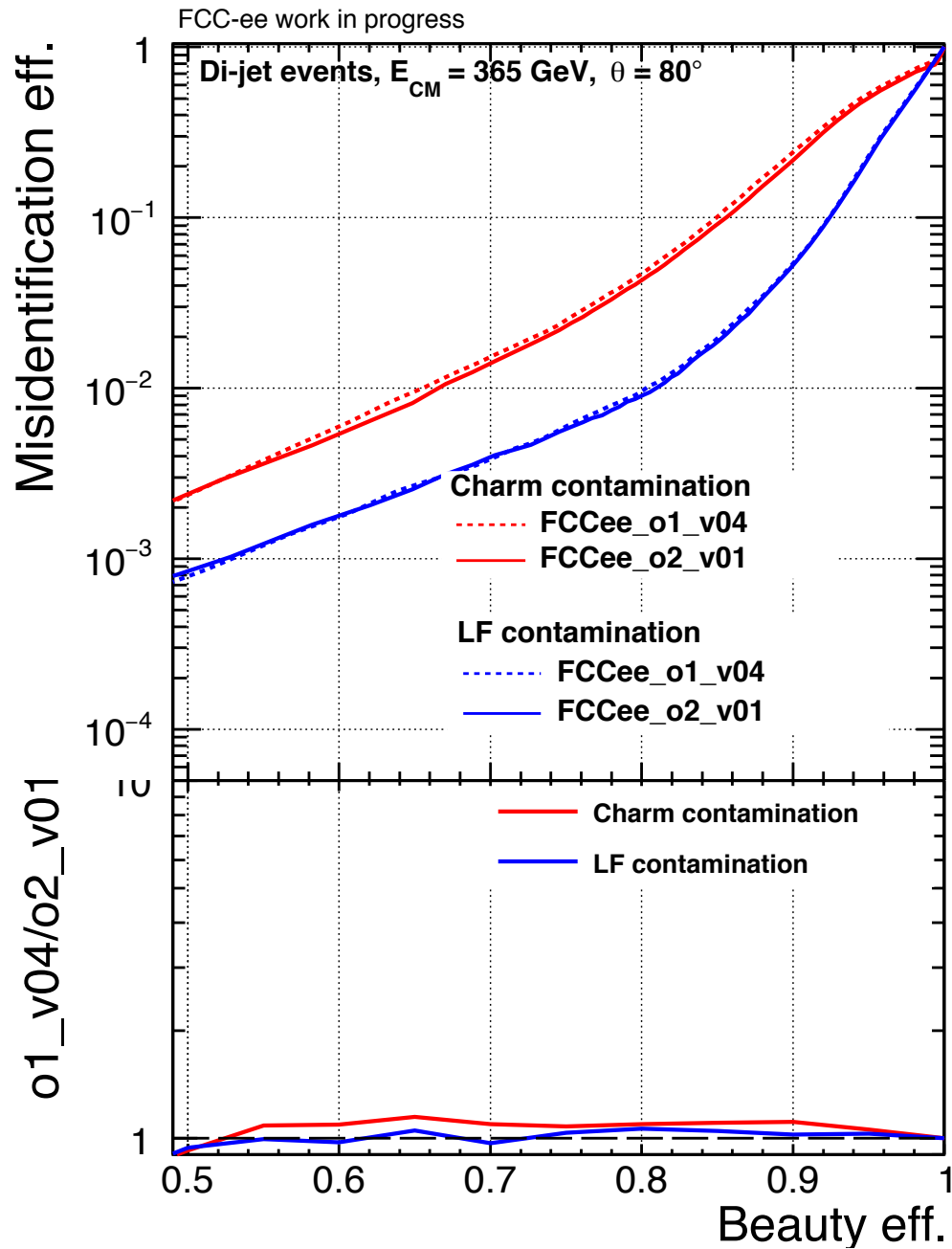


Flavour tagging for dijets at 365 GeV



- ✦ Flavour tagging relies on the capability of primary and secondary vertices reconstruction
=> expected to improve with a vertex detector closer to the interaction point
- ✦ Results obtained in full detector simulation and reconstruction
- ✦ Dijet events with $E_{cm} = 365$ GeV and $\theta = 80$ deg

dashed = CDR
solid = post-CDR



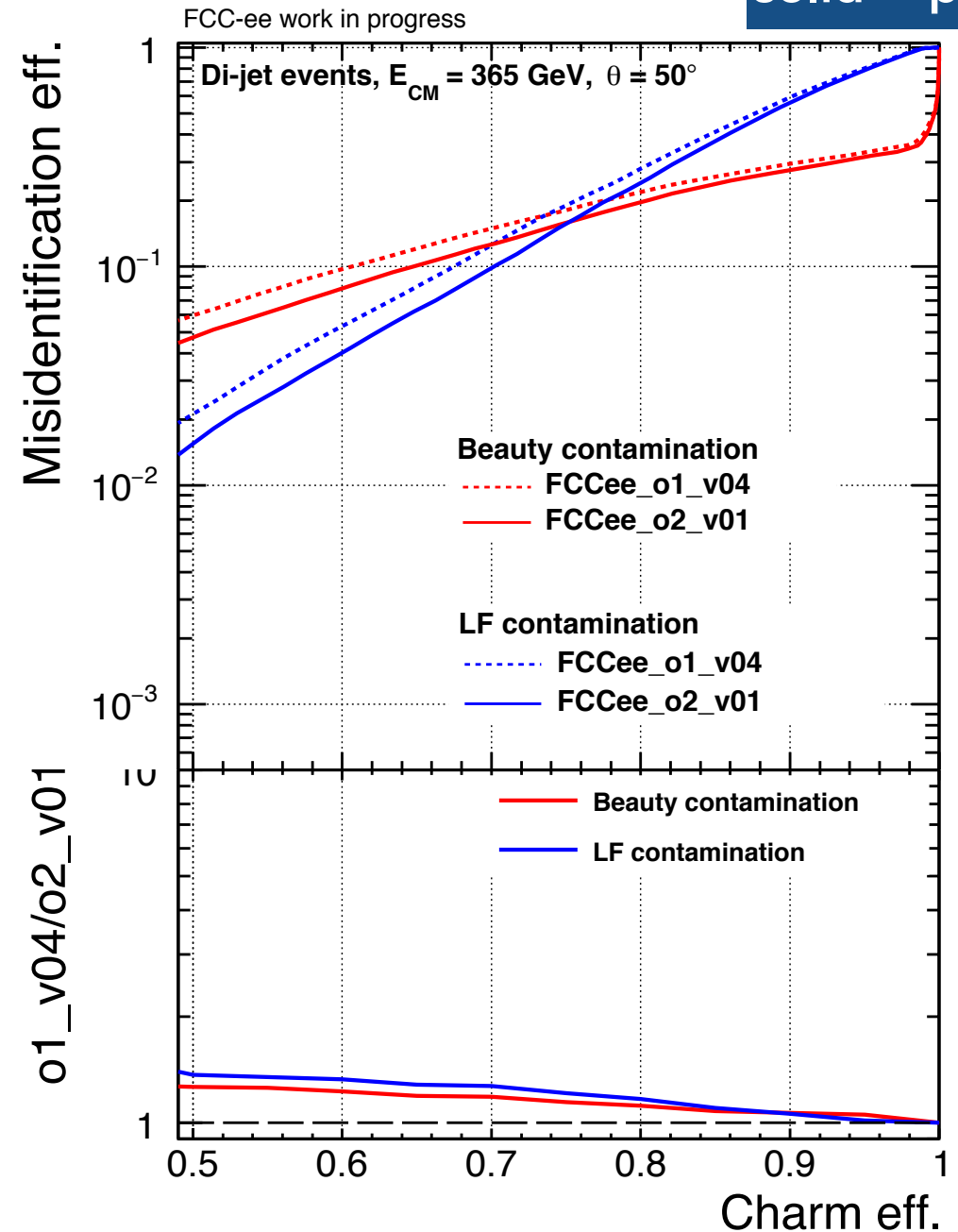
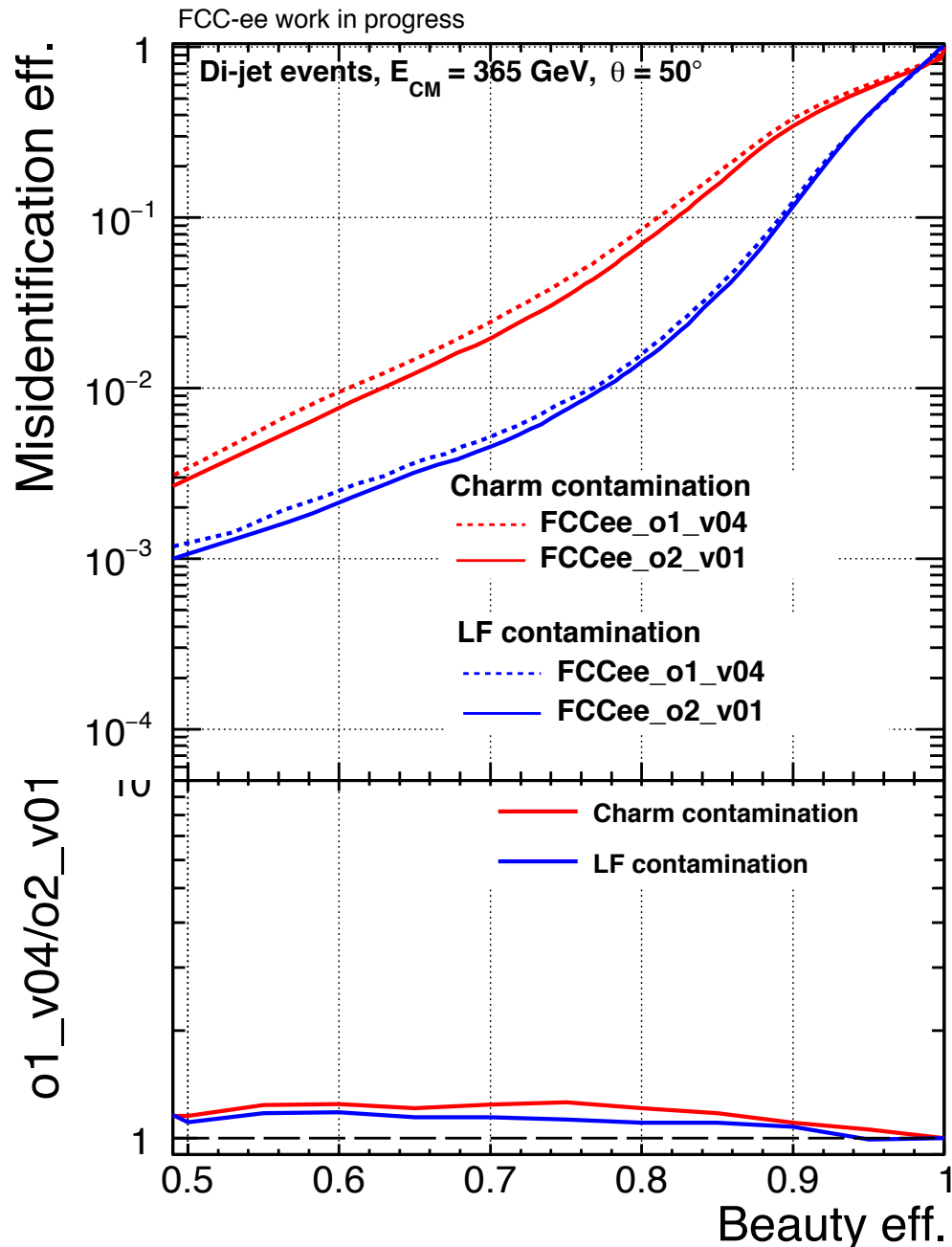


Flavour tagging for dijets at 365 GeV



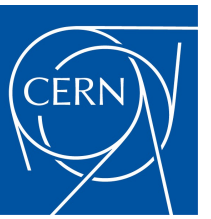
- ✦ Flavour tagging relies on the capability of primary and secondary vertices reconstruction
=> expected to improve with a vertex detector closer to the interaction point
- ✦ Results obtained in full detector simulation and reconstruction
- ✦ Dijet events with $E_{cm} = 365$ GeV and $\theta = 50$ deg

dashed = CDR
solid = post-CDR



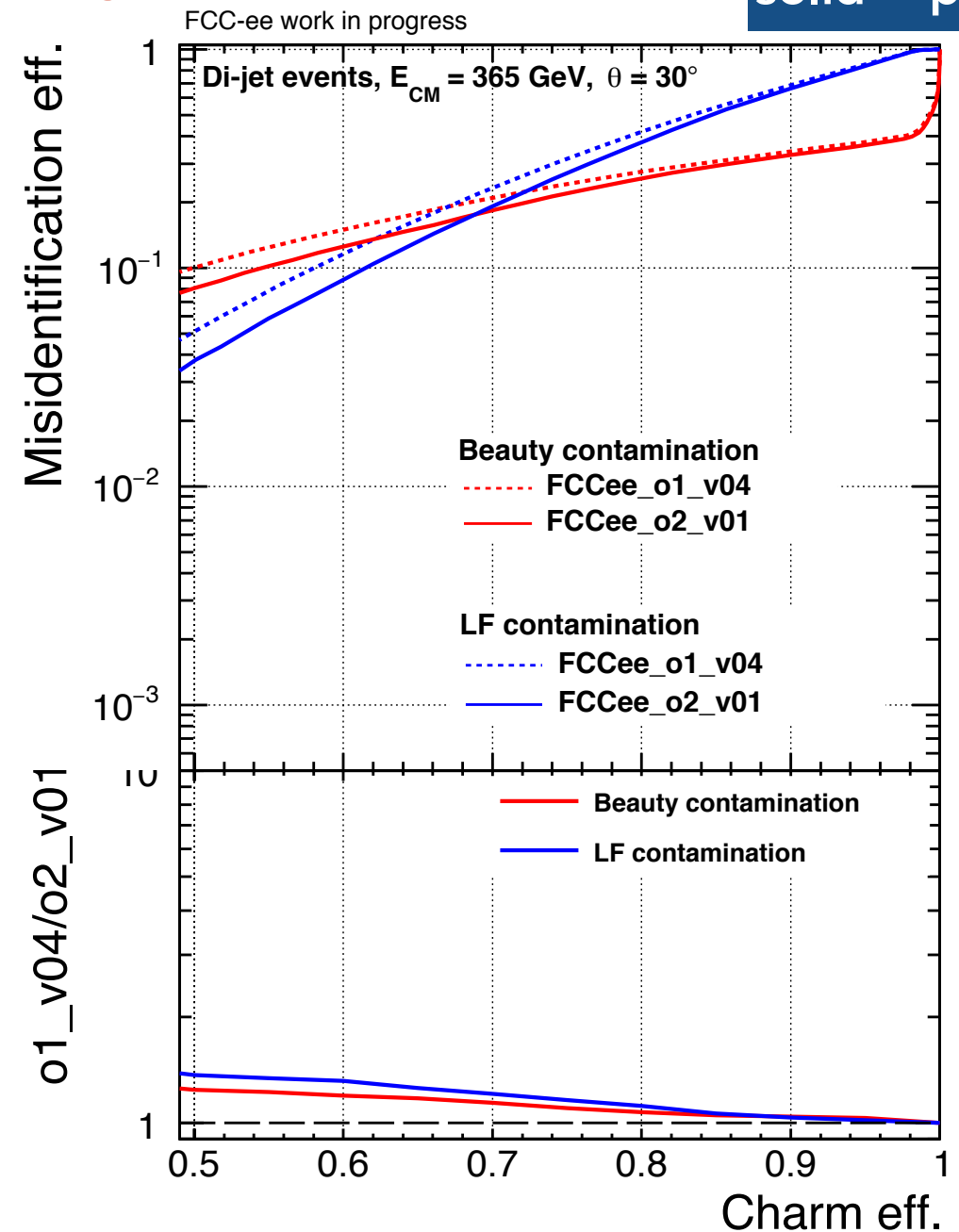
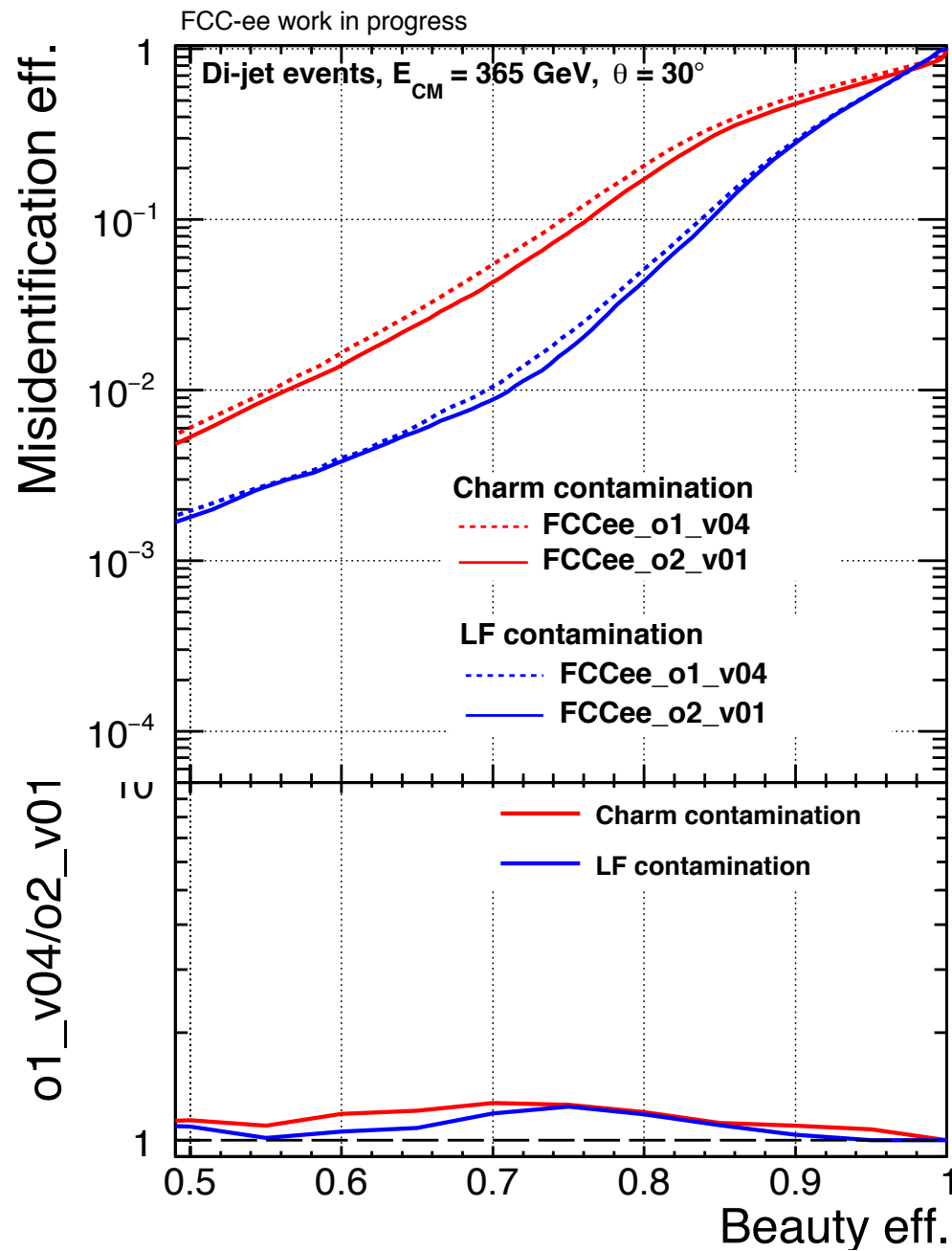


Flavour tagging for dijets at 365 GeV



- ✦ Flavour tagging relies on the capability of primary and secondary vertices reconstruction
=> expected to improve with a vertex detector closer to the interaction point
- ✦ Results obtained in full detector simulation and reconstruction
- ✦ Dijet events with $E_{cm} = 365$ GeV and $\theta = 30$ deg

dashed = CDR
solid = post-CDR



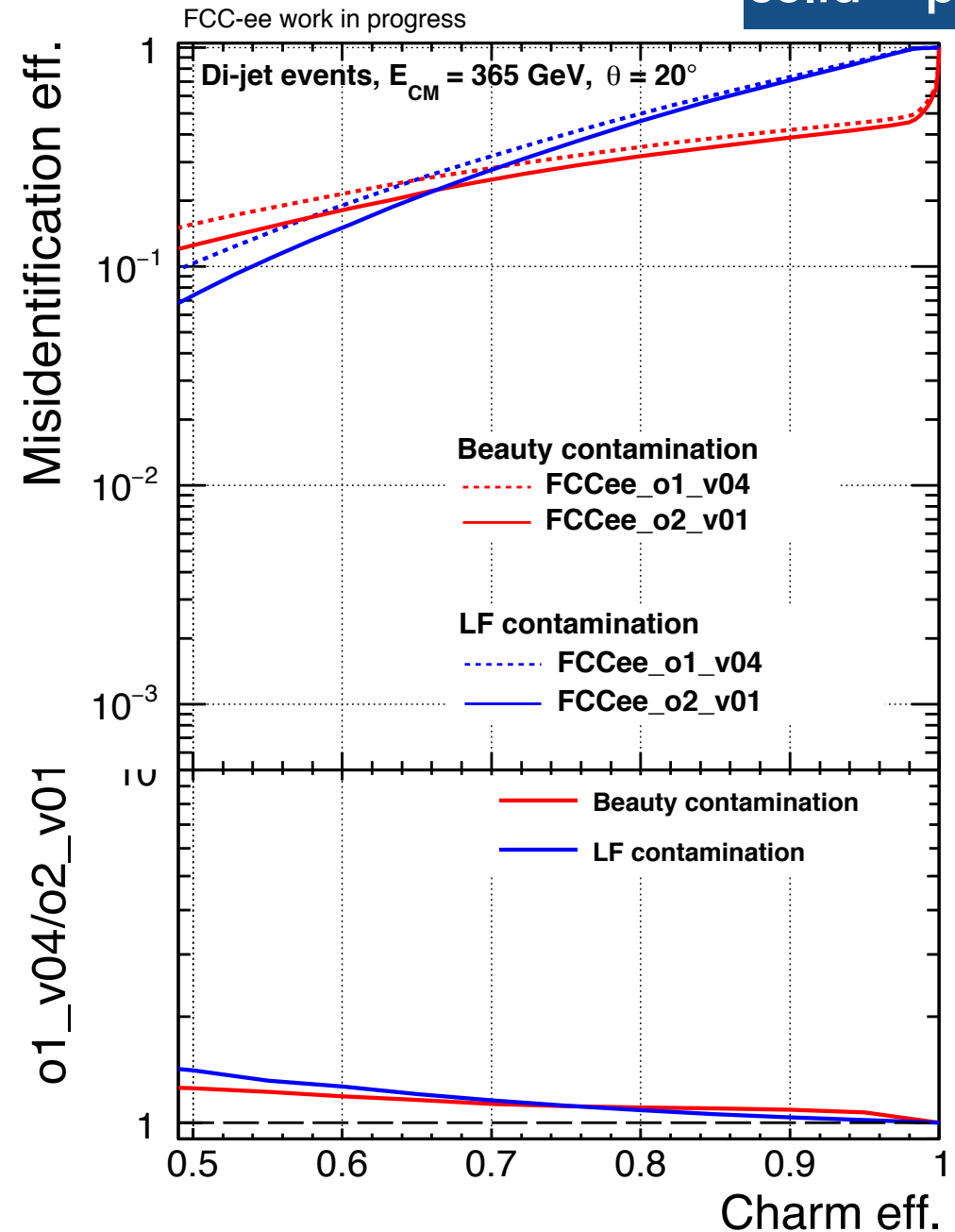
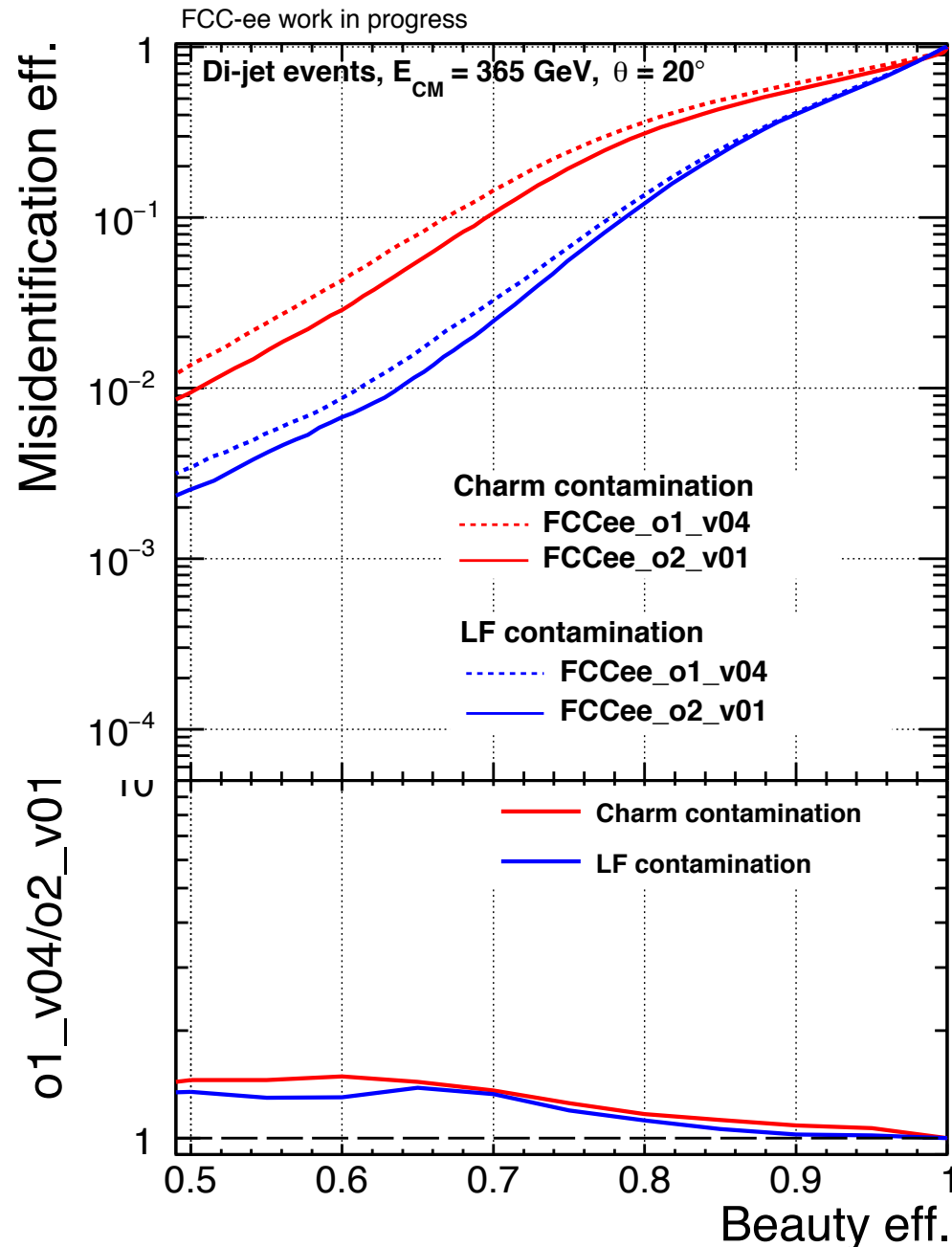


Flavour tagging for dijets at 365 GeV



- ◆ Flavour tagging relies on the capability of primary and secondary vertices reconstruction
=> expected to improve with a vertex detector closer to the interaction point
- ◆ Results obtained in full detector simulation and reconstruction
- ◆ Dijet events with $E_{cm} = 365$ GeV and $\theta = 20$ deg

dashed = CDR
solid = post-CDR



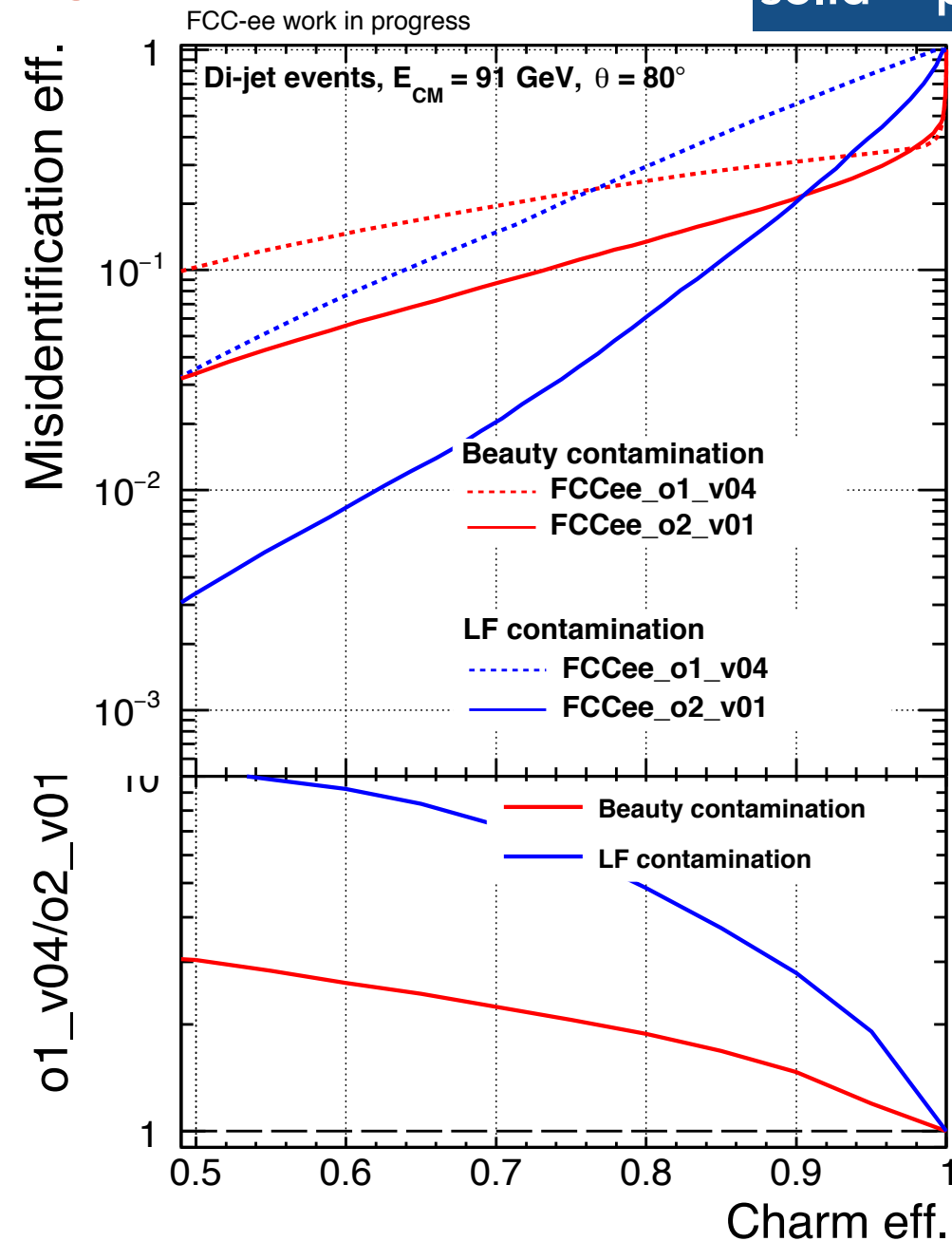
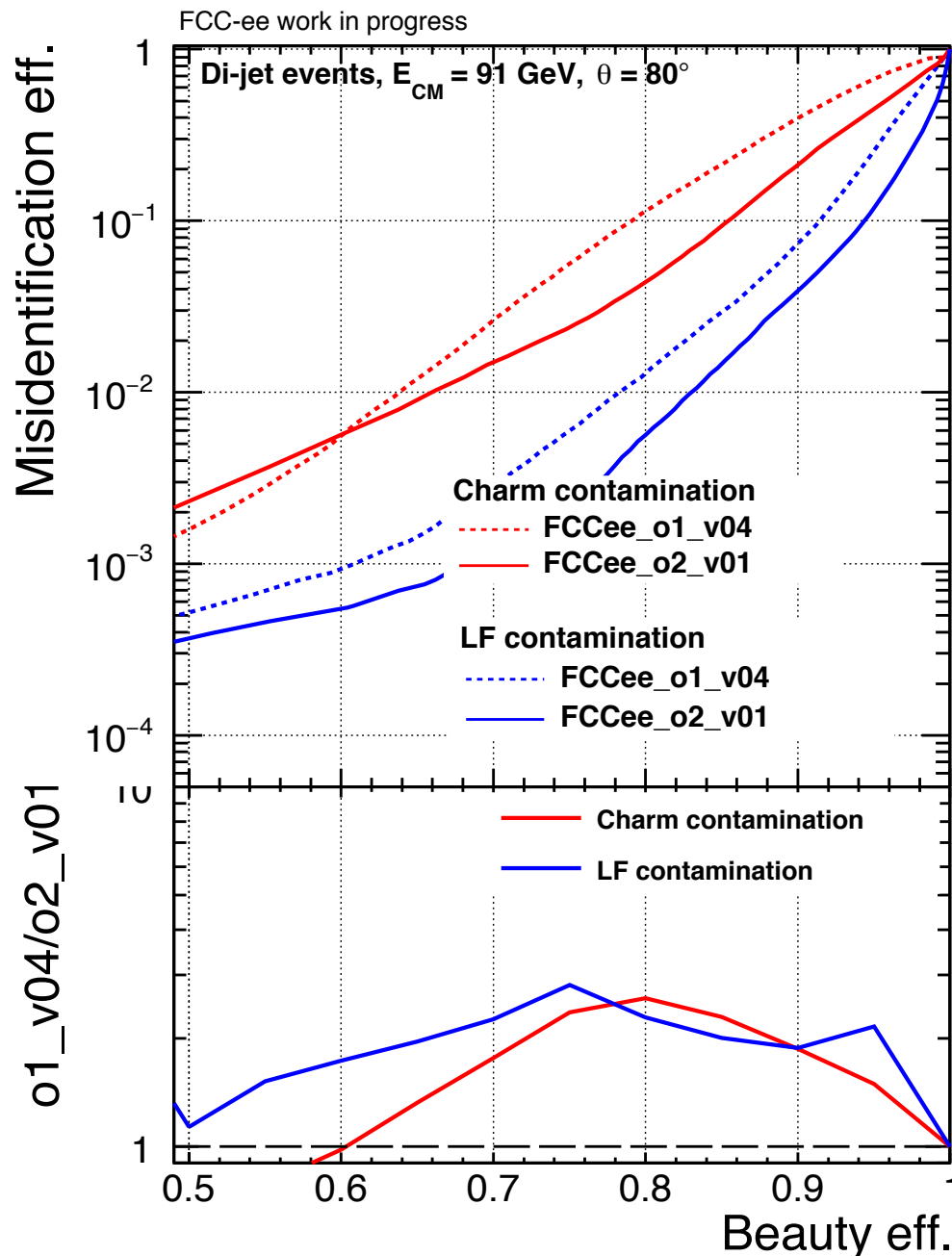


Flavour tagging for dijets at 91 GeV



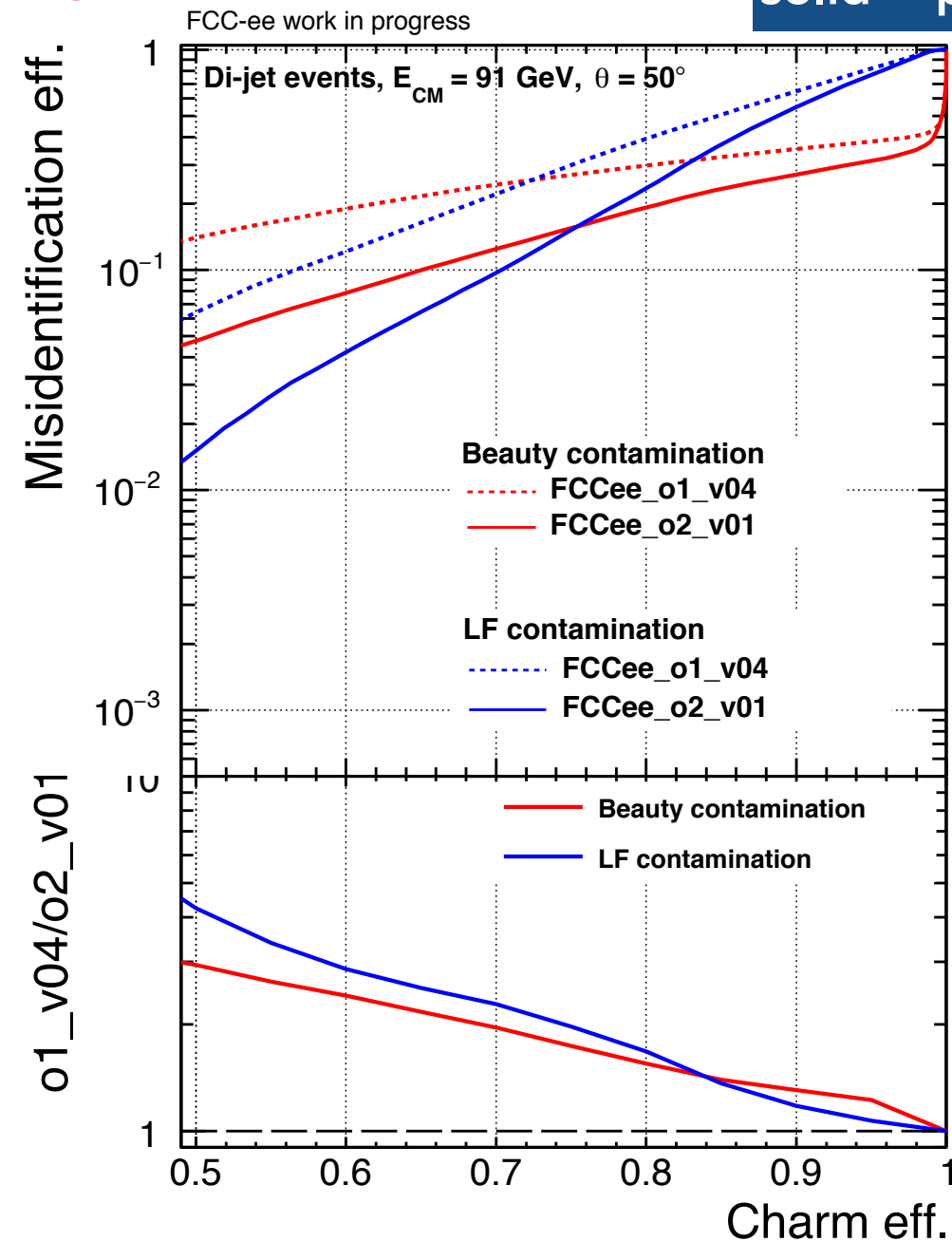
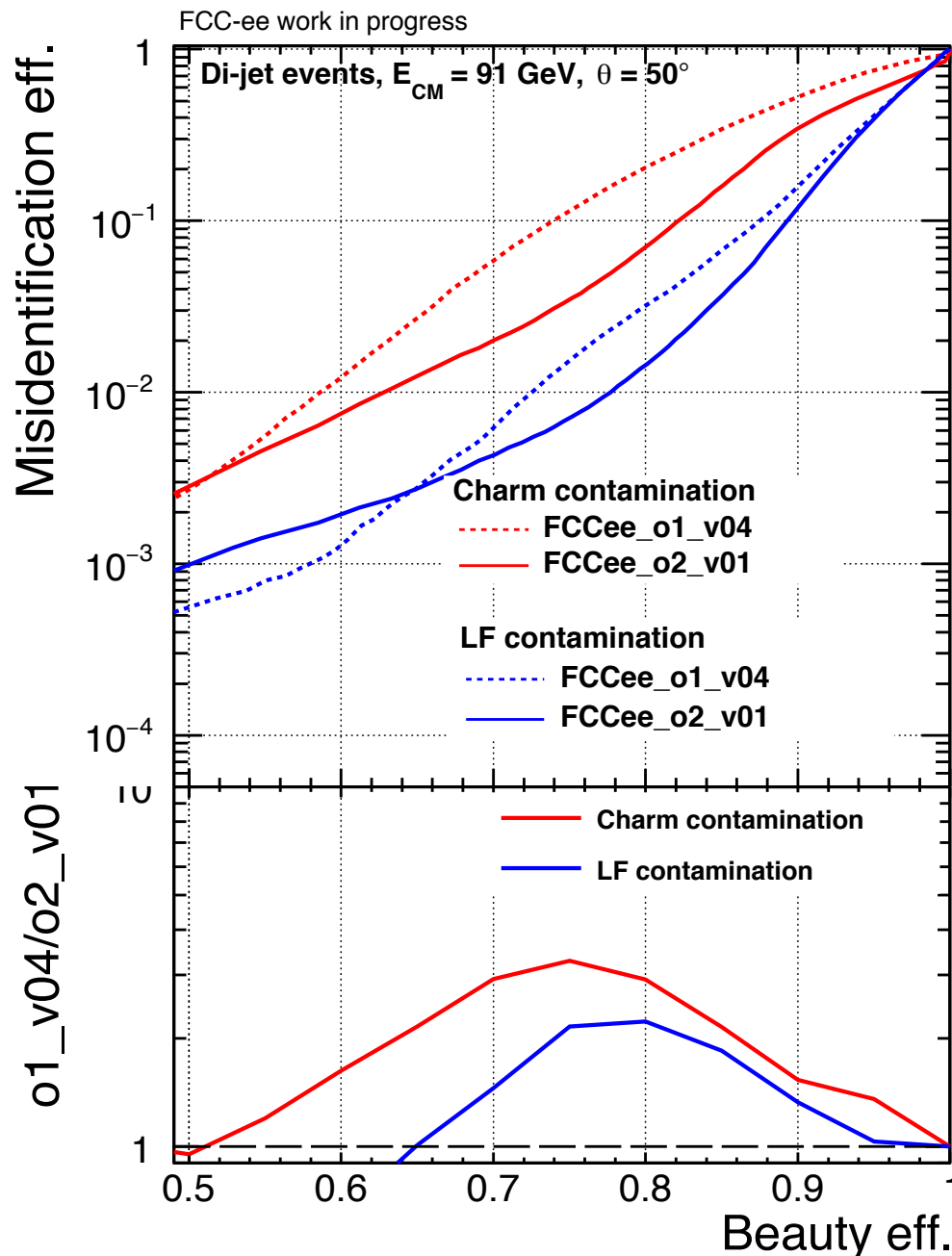
- ✦ Flavour tagging relies on the capability of primary and secondary vertices reconstruction
=> expected to improve with a vertex detector closer to the interaction point
- ✦ Results obtained in full detector simulation and reconstruction
- ✦ Dijet events with $E_{cm} = 91$ GeV and $\theta = 80$ deg

dashed = CDR
solid = post-CDR



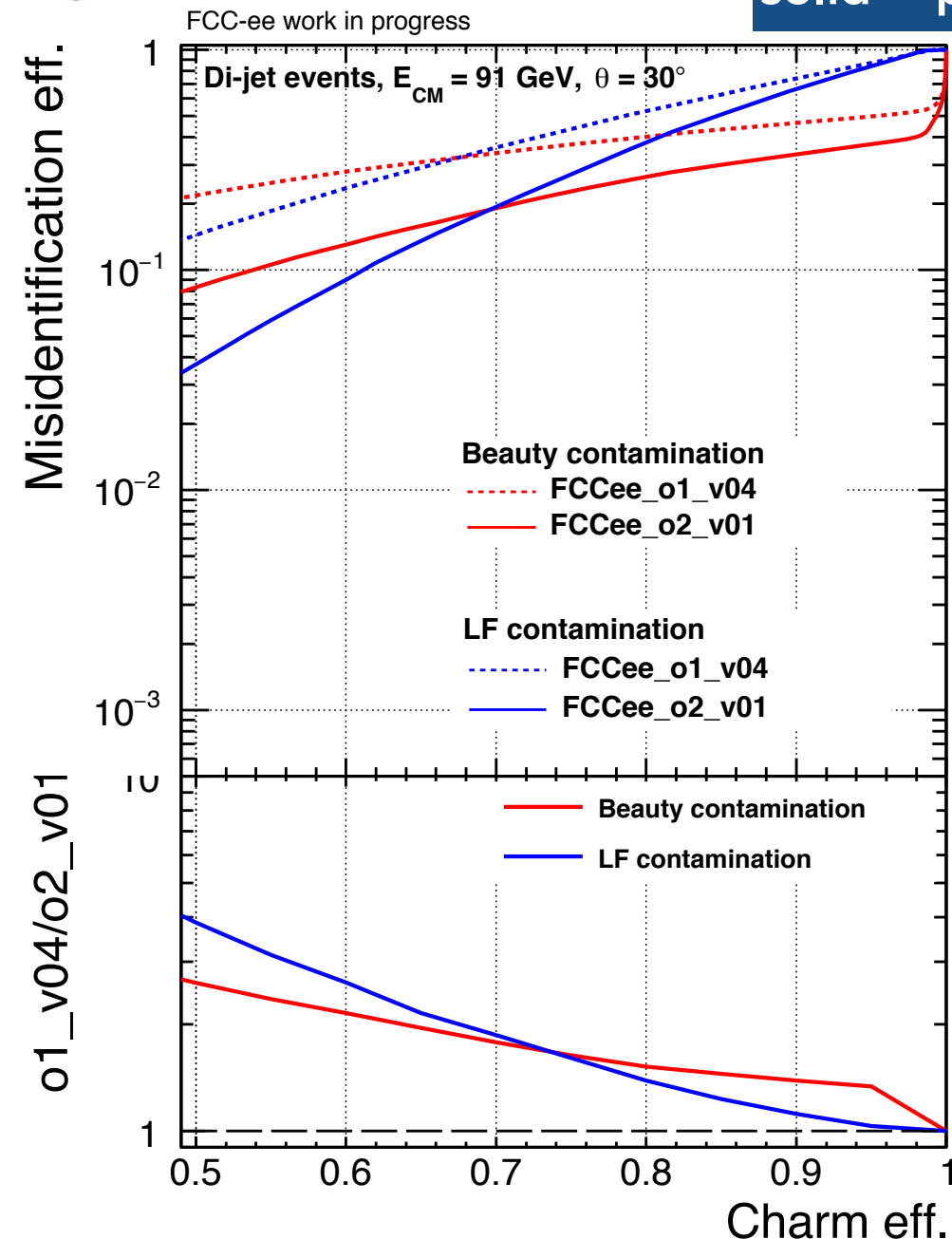
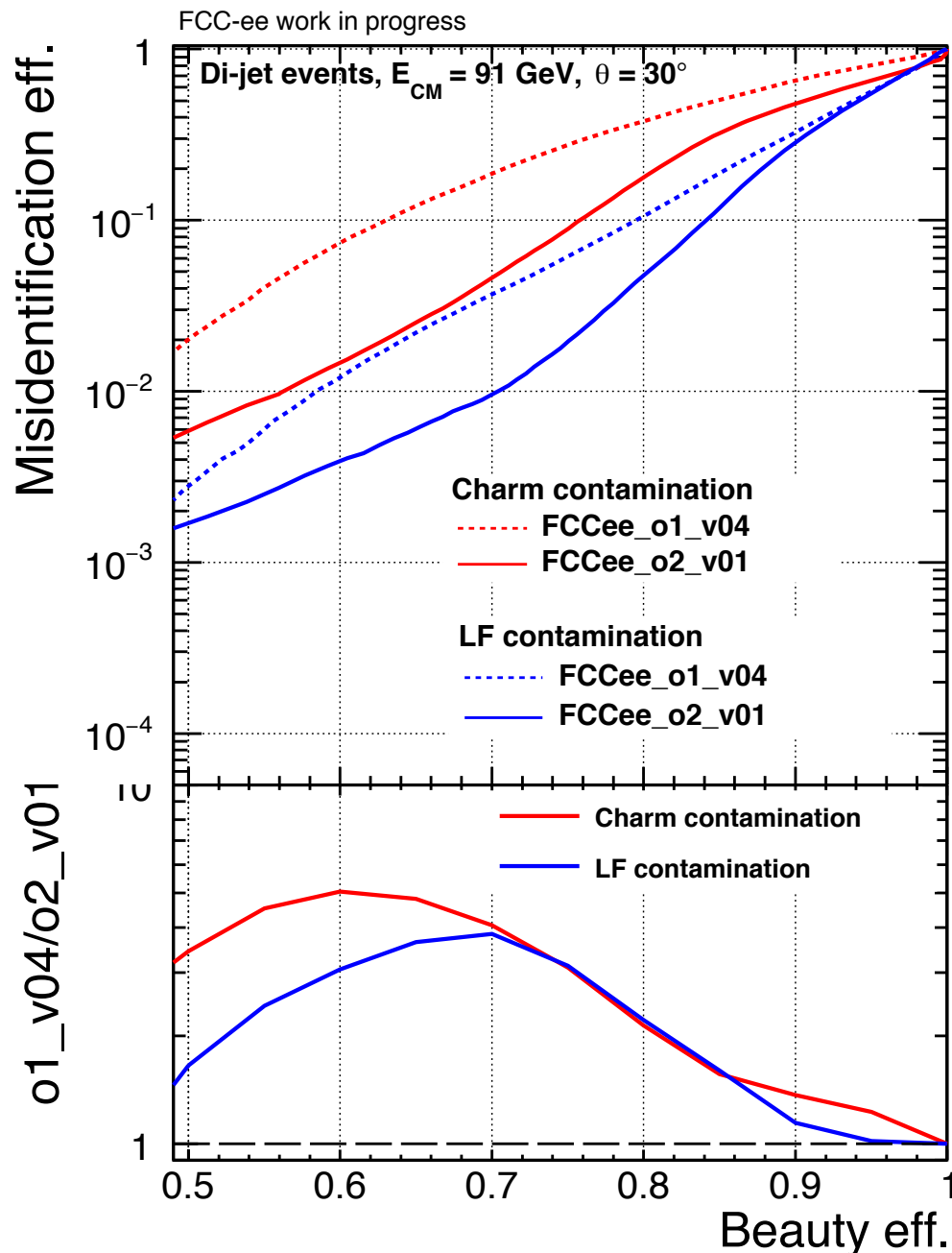
- ✦ Flavour tagging relies on the capability of primary and secondary vertices reconstruction
=> expected to improve with a vertex detector closer to the interaction point
- ✦ Results obtained in full detector simulation and reconstruction
- ✦ Dijet events with $E_{cm} = 91$ GeV and $\theta = 50$ deg

dashed = CDR
solid = post-CDR



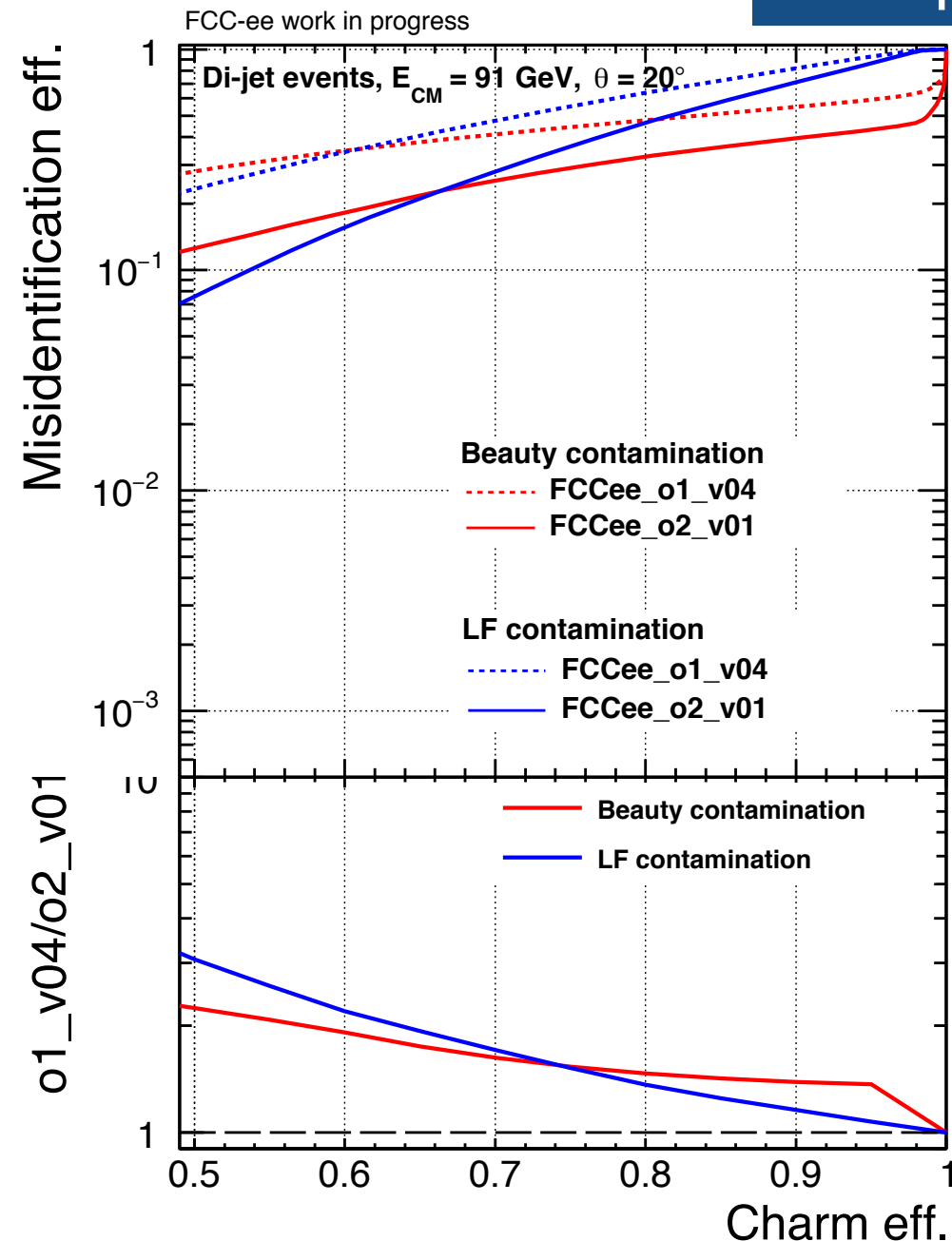
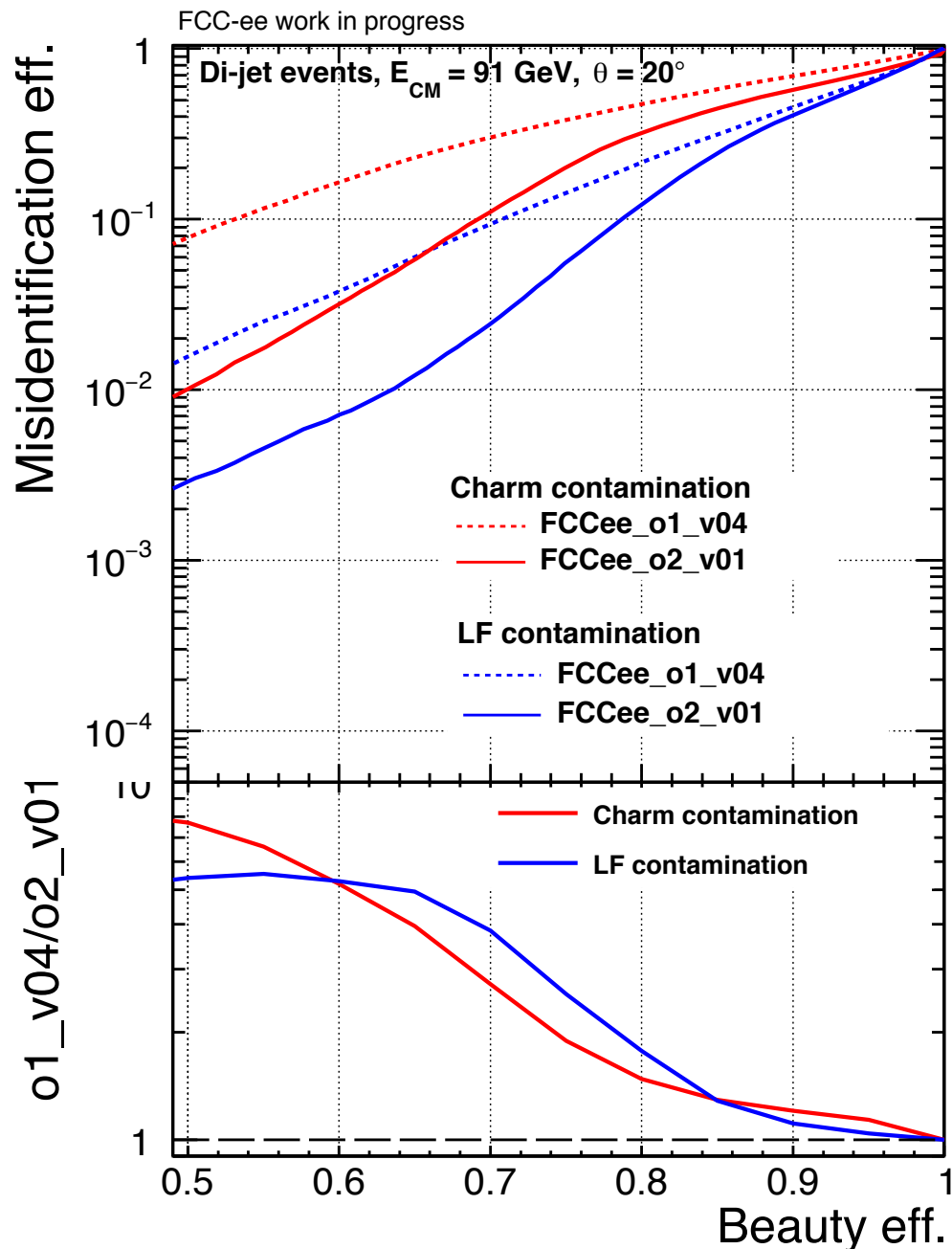
- ✦ Flavour tagging relies on the capability of primary and secondary vertices reconstruction
=> expected to improve with a vertex detector closer to the interaction point
- ✦ Results obtained in full detector simulation and reconstruction
- ✦ Dijet events with $E_{cm} = 91$ GeV and $\theta = 30$ deg

dashed = CDR
solid = post-CDR



- ✦ Flavour tagging relies on the capability of primary and secondary vertices reconstruction
=> expected to improve with a vertex detector closer to the interaction point
- ✦ Results obtained in full detector simulation and reconstruction
- ✦ Dijet events with $E_{cm} = 91$ GeV and $\theta = 20$ deg

dashed = CDR
solid = post-CDR





Preliminary observations



- ◆ **Flavour tagging** in dijet events at **365 GeV** improves **slightly** with post-CDR model
- ◆ **Flavour tagging** in dijet events at **91 GeV** improves **significantly** with post-CDR model
 - ◆ @365 GeV, the polar angle dependence shows that the improvement:
 - ◆ is better in the forward direction for the b-tagging
 - ◆ is similar in the forward and central direction for the c-tagging
 - ◆ @91 GeV, the polar angle dependence shows that the improvement:
 - ◆ is better in the forward direction for the b-tagging
 - ◆ is better in the central direction for the c-tagging

- ◆ **Flavour tagging** in dijet events at **365 GeV** improves **slightly** with post-CDR model
- ◆ **Flavour tagging** in dijet events at **91 GeV** improves **significantly** with post-CDR model
 - ◆ @365 GeV, the polar angle dependence shows that the improvement:
 - ◆ is better in the forward direction for the b-tagging
 - ◆ is similar in the forward and central direction for the c-tagging
 - ◆ @91 GeV, the polar angle dependence shows that the improvement:
 - ◆ is better in the forward direction for the b-tagging
 - ◆ is better in the central direction for the c-tagging

Food for thoughts

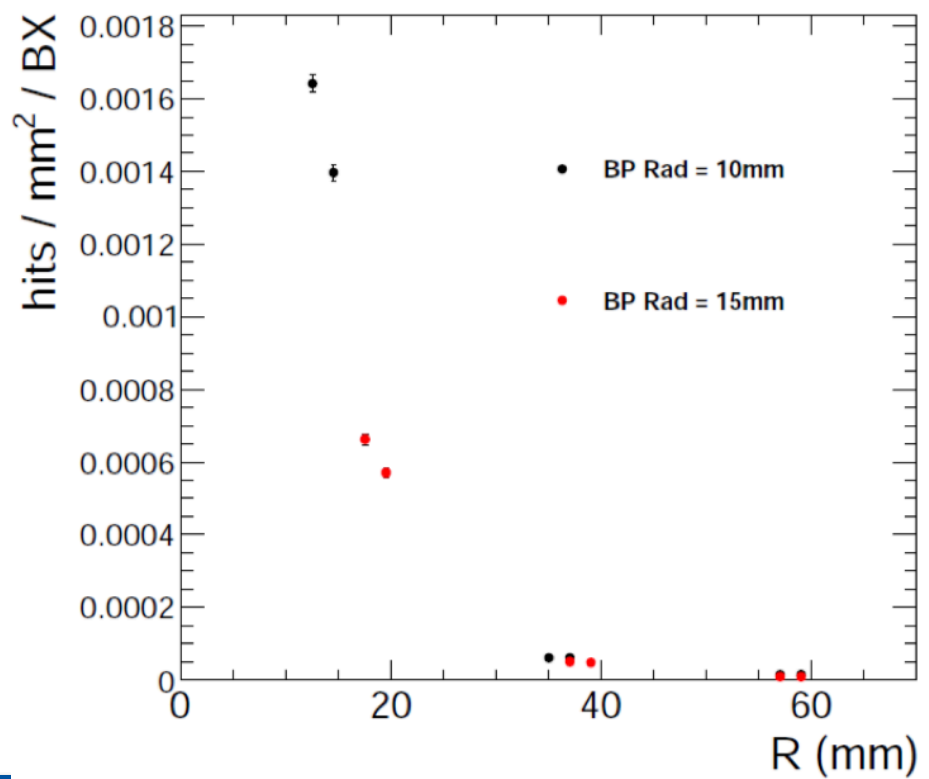
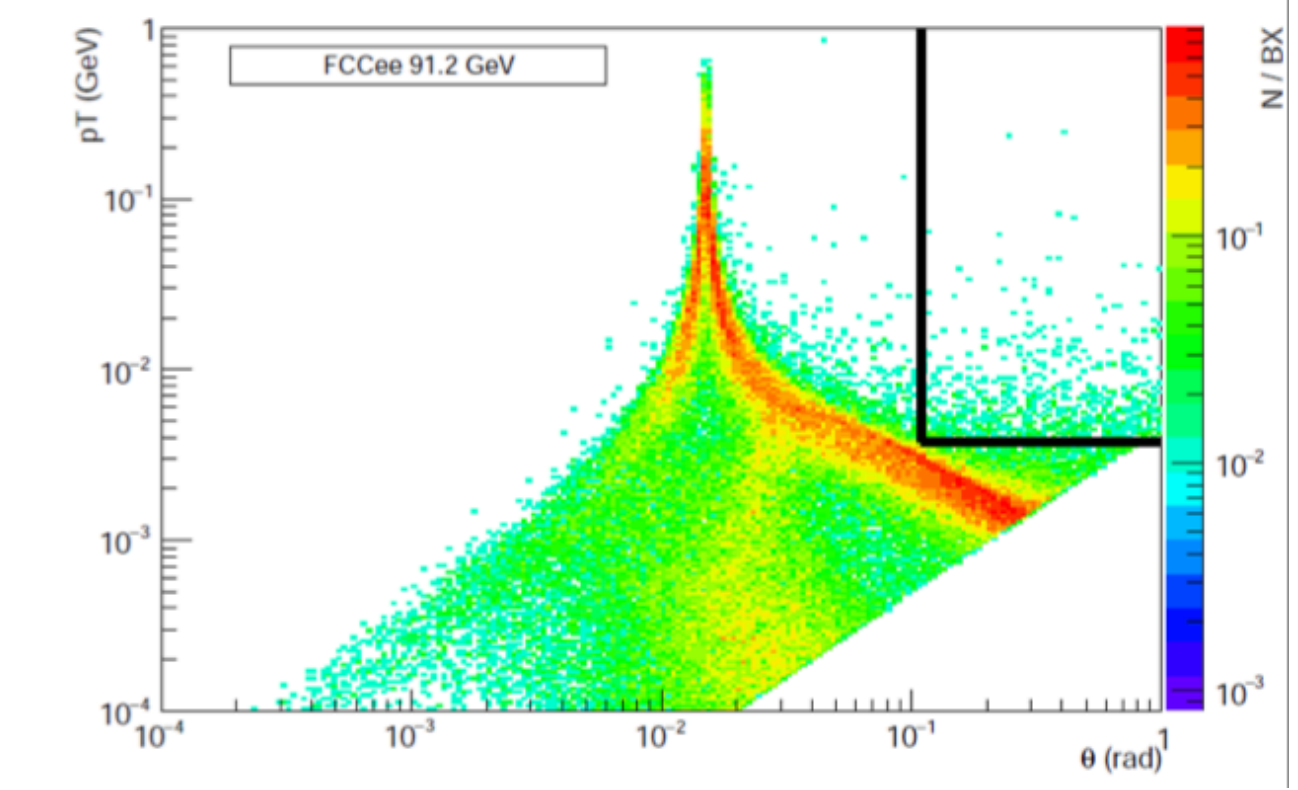
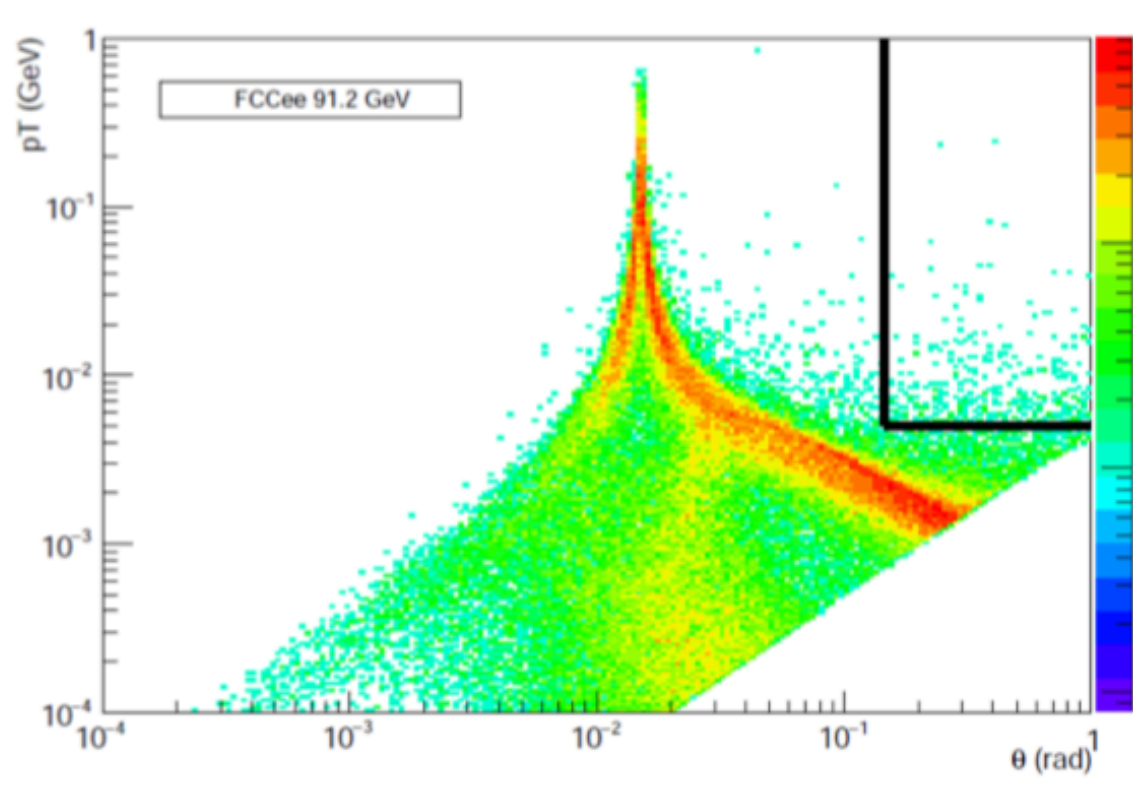
- ◆ b tagging
 - ◆ improvement stronger at 91GeV than at 365GeV \leq fraction of b hadrons that decay after the innermost layer is smaller at 91GeV than at 365GeV
 - ◆ @91GeV && 90deg: ~10%, @365GeV && 90deg: ~50%
 - ◆ improvement stronger in the forward than in the central region at both energies \leq fraction of b hadrons that decay after the innermost layer is smaller at 20deg than at 80deg
- ◆ tagging depends on many other variables: vertex mass, vertex resolution, impact parameter significance, ... This is only the start of the investigation



Incoherent pairs background



- ◆ distribution of produced particles from incoherent pairs @91 GeV
-
- ◆ old model
- ◆ new model (smaller beampipe)



- ◆ occupancy in the barrel layers
 - ◆ old model x 50BX < 4x10⁻⁴
 - ◆ new model x 50BX < 8x10⁻⁴
- => still acceptable



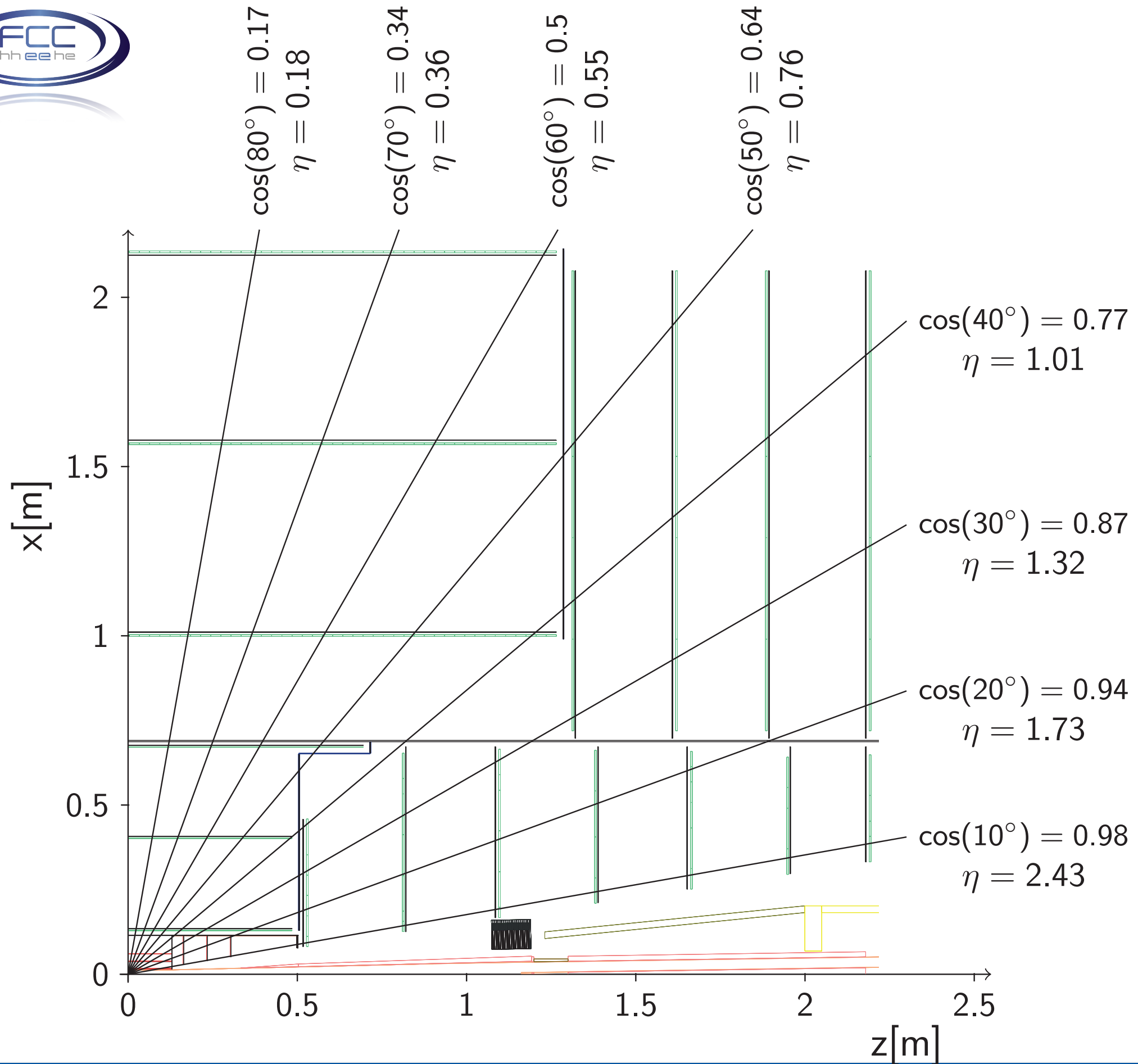
Summary



- ◆ A new design for the **CLD** detector (**post-CDR**) has been realized for a new FCC-ee interaction region with a reduced beam pipe radius (15 mm \rightarrow 10 mm) at the IP
 - ◆ **vertex barrel closer to interaction point**
- ◆ A very first look at the performance of the post-CDR CLD detector compared with the CDR model
 - ◆ The **impact parameter resolutions improve**, especially for low momentum tracks
 - ◆ The transverse momentum resolution is unaffected (not shown in the talk)
 - ◆ The **flavour tagging capabilities improve**
 - ◆ **slightly for 365 GeV, strongly for 91 GeV**
 - ◆ with a dependence on polar angle observed
- ◆ Next step: analysis the flavour tagging results case by case
 - ◆ vertexing performance, jet clustering and classification
 - ◆ thorough investigation of the input variables to the BDT necessary
 - ◆ + *part of the problem is the long time for full simulation; place where fast sim tool would be extremely helpful*
- ◆ Next² step: study effect of the background in the detector performance
 - ◆ from preliminary study: incoherent pairs do not seem to represent an issue



Extra



LFCIPlus vertex finder algorithm

◆ Vertex Fitter for Primary Vertex

- ◆ if beam spot is constrained, beam spot centre as initial 3D point
- ◆ 3D fit performed for the vertex position by adding χ^2 contribution from each track; tracks with highest χ^2 and above a threshold are removed
- ◆ *output*: minimized χ^2 , vertex uncertainty and probability, tracks associated to PV

◆ Vertex Fitter for Secondary Vertices

- ◆ tracks not associated to the PV are paired and used as seeds for the SVs
- ◆ 3D fit performed for the vertex position by adding χ^2 contribution from each track pair; tracks with highest χ^2 and above a threshold are removed + additional selection criteria (e.g. V^0 discarded)
- ◆ additional tracks are added to the SV and accepted if χ^2 contribution below threshold
- ◆ at this point: tracks may have been used for more than one vertex
- ◆ to remove overlap: vertices are scanned in order of probability (high to low) and number of tracks (3 to 2); tracks associated to vertices are removed from further SVs
- ◆ *output*: minimized χ^2 , vertices uncertainty and probability, tracks associated to SVs



Tracks association

◆ Classification of tracks for vertex finder performance

- ◆ *Primary*: tracks originated from the primary vertex
- ◆ *Bottom*: tracks whose most immediate parent with a non-zero lifetime contains a b quark
- ◆ *Charm*: tracks whose most immediate parent with a non-zero lifetime contains a c quark
- ◆ *Others*: all other tracks (τ decays, strange hadrons, photon conversions, ...)



Name	Description	Normalization factor	Used by category
trk1d0sig	d0 significance of track with highest d0 significance	1	A, B, C, D
trk2d0sig	d0 significance of track with second highest d0 significance	1	A, B, C, D
trk1z0sig	z0 significance of track with highest d0 significance	1	A, B, C, D
trk2z0sig	z0 significance of track with second highest d0 significance	1	A, B, C, D
trk1pt	transverse momentum of track with highest d0 significance	$1/E_{jet}$	A, B, C, D
trk2pt	transverse momentum of track with second highest d0 significance	$1/E_{jet}$	A, B, C, D
jprobr	joint probability in the r-phi plane using all tracks	1	A, B, C, D
jprobr5sigma	joint probability in the r-phi plane using all tracks having impact parameter significance exceeding 5 sigma	1	A, B, C, D
jprobz	joint probability in the z projection using all tracks	1	A, B, C, D
jprobz5sigma	joint probability in the z projection using all tracks having impact parameter significance exceeding 5 sigma	1	A, B, C, D
d0bprob	product of b-quark probabilities of d0 values for all tracks, using b/c/q d0 distributions	1	A, B, C, D
d0cprob	product of c-quark probabilities of d0 values for all tracks, using b/c/q d0 distributions	1	A, B, C, D
d0qprob	product of q-quark probabilities of d0 values for all tracks, using b/c/q d0 distributions	1	A, B, C, D
z0bprob	product of b-quark probabilities of z0 values for all tracks, using b/c/q z0 distributions	1	A, B, C, D
z0cprob	product of c-quark probabilities of z0 values for all tracks, using b/c/q z0 distributions	1	A, B, C, D
z0qprob	product of q-quark probabilities of z0 values for all tracks, using b/c/q z0 distributions	1	A, B, C, D
nmuon	number of identified muons	1	A, B, C, D
nelectron	number of identified electrons	1	A, B, C, D
trkmass	mass of all tracks exceeding 5 sigma significance in d0/z0 values	1	A, B, C, D



Name	Description	Normalization factor	Used by category
1vtxprob	vertex probability with all tracks associated in vertices combined	1	B, C, D
vtxlen1	decay length of the first vertex in the jet (zero if no vertex is found)	$1/E_{\text{jet}}$	B, C, D
vtxlen2	decay length of the second vertex in the jet (zero if number of vertex is less than two)	$1/E_{\text{jet}}$	D
vtxlen12	distance between the first and second vertex (zero if number of vertex is less than two)	$1/E_{\text{jet}}$	D
vtxsig1	decay length significance of the first vertex in the jet (zero if no vertex is found)	$1/E_{\text{jet}}$	B, C, D
vtxsig2	decay length significance of the second vertex in the jet (zero if number of vertex is less than two)	$1/E_{\text{jet}}$	D
vtxsig12	vtxlen12 divided by its error as computed from the sum of the covariance matrix of the first and second vertices, projected along the line connecting the two vertices	$1/E_{\text{jet}}$	D
vtxdirang1	the angle between the momentum (computed as a vector sum of track momenta) and the displacement of the first vertex	E_{jet}	B, C, D
vtxdirang2	the angle between the momentum (computed as a vector sum of track momenta) and the displacement of the second vertex	E_{jet}	D
vtxmult1	number of tracks included in the first vertex (zero if no vertex is found)	1	B, C, D
vtxmult2	number of tracks included in the second vertex (zero if number of vertex is less than two)	1	D
vtxmult	number of tracks which are used to form secondary vertices (summed for all vertices)	1	D
vtxmom1	magnitude of the vector sum of the momenta of all tracks combined into the first vertex	$1/E_{\text{jet}}$	B, C, D
vtxmom2	magnitude of the vector sum of the momenta of all tracks combined into the second vertex	$1/E_{\text{jet}}$	D
vtxmass1	mass of the first vertex computed from the sum of track four-momenta	1	B, C, D
vtxmass2	mass of the second vertex computed from the sum of track four-momenta	1	D
vtxmass	vertex mass as computed from the sum of four momenta of all tracks forming secondary vertices	1	B, C, D
vtxmasspc	mass of the vertex with minimum pt correction allowed by the error matrices of the primary and secondary vertices	1	B, C, D
vtxprob	vertex probability; for multiple vertices, the probability P is computed as $1-P = (1-P_1)(1-P_2)\dots(1-P_N)$	1	B, C, D